

## Experimental Measurement of Neoclassical Mobility in an Annular Malmberg-Penning Trap

Joe Espejo, Qudsia Quraishi, and Scott Robertson

*Department of Physics, University of Colorado, Boulder, Colorado 80309-0390*

(Received 1 March 2000)

An annular Malmberg-Penning trap confining a non-neutral plasma of electrons has been operated with an azimuthal magnetic field to create drifts orthogonal to the magnetic flux surfaces. An applied electric field and collisions with added helium drive transport by electric mobility. The measured confinement times have the expected neoclassical magnetic-field dependence, are approximately 0.8 of the value based upon the neoclassical mobility, and differ from the classical value by more than a factor of 3 at the highest value of azimuthal field.

PACS numbers: 52.25.Wz, 52.25.Fi, 52.55.Dy

In fusion devices with toroidal fields, neoclassical transport is greater than classical transport in a uniform field of the same strength as a result of gradient and curvature drifts that are orthogonal to the flux surfaces [1,2]. We describe neoclassical transport experiments with an annular Malmberg-Penning trap in which a current-carrying conductor has been added on the axis to create an azimuthal magnetic field in addition to the usual axial field [3,4]. At the ends of the device, electrons are reflected by an electrostatic field and there is a small radial displacement, orthogonal to the cylindrical flux surfaces, from the  $\mathbf{E} \times \mathbf{B}$  drift. These displacements are in opposite directions at the two ends of the device and give the drift orbits a finite radial extent. The drift orbit is cucumberlike when projected onto the  $r$ - $z$  plane and is analogous to the banana orbits of the tokamak. Collisions with neutral gas result in an orbit being displaced by approximately the drift orbit width rather than the Larmor radius. Thus transport coefficients for the annular trap [5] have the neoclassical value rather than the classical value. The Malmberg-Penning [6] trap in its standard form has been used for detailed studies of transport arising from electron-electron and electron-neutral [7] collisions. In the experiments reported here, a radial electric field is applied which makes mobility the dominant source of particle transport, and the measured mobility is shown to agree, approximately, with the neoclassical value, to have the neoclassical dependence upon each of the magnetic fields, and to be inconsistent with the classical value. Neoclassical diffusion is more important than mobility in determining the performance of fusion devices; however, mobility may be an issue in those fusion plasma devices where a strong electric field is applied at the edge to modify transport [8,9]. Currents driven by neoclassical effects have been measured in a toroidal octupole device [10] and diffusion of ions approaches the neoclassical value in tokamaks operated in advanced modes that reduce turbulence [11–14].

A simplified version of the trap geometry is shown in Fig. 1, which illustrates the similarity of the drift orbits to those of the tokamak. The plasma is contained

between concentric cylinders 150 mm in length of radii  $r_1 = 25.4$  mm and  $r_2 = 48$  mm. There are Helmholtz coils for creating an axial field,  $B_z$ , of 0–18 mT and conductors along the axis to create an azimuthal field,  $B_\theta$ , of 0–12 mT. A field line near the inner cylinder spirals approximately once around the axis when these two magnetic

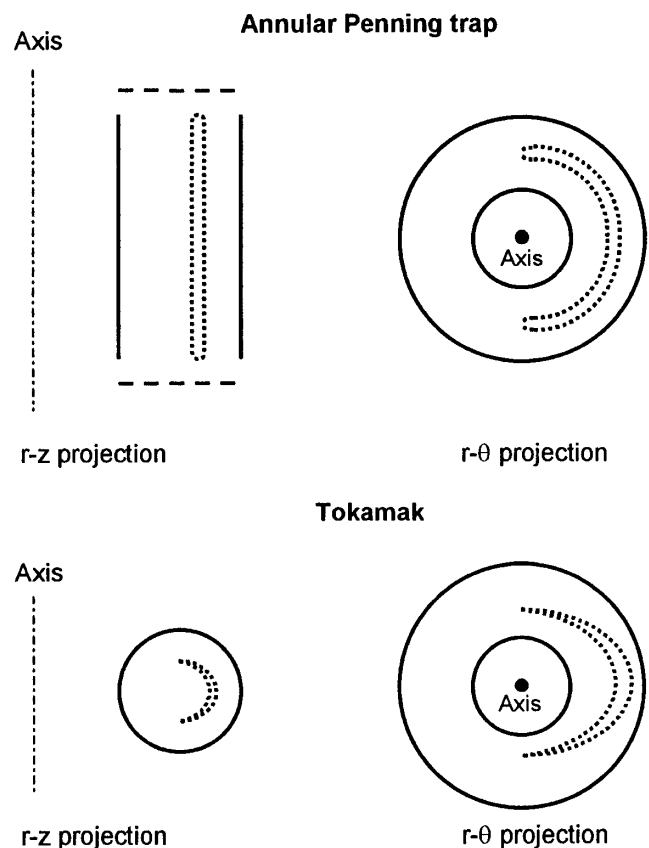


FIG. 1. Comparison of drift orbits (dotted lines) in the tokamak and the annular trap. The upper figure shows the concentric cylindrical walls of the annular trap with the oval drift orbit. The lower figure shows the toroidal walls of the tokamak with the bananalike drift orbit. The left side is an  $r$ - $z$  projection and the right side is an  $r$ - $\theta$  projection. The devices have cylindrical symmetry.

fields are equal. Electrons are electrostatically reflected at the ends of the cylinders by a negative potential,  $-6$  V, applied to annular grids. Mobility transport is driven by a radial electric field within the cylinders created by a positive bias potential,  $U = 36$  V, applied to the outer cylinder. The space charge electric field of the confined electrons is a small perturbation. The inner electrode is kept at ground potential. At one end of the device there is a filament, not shown, biased to  $-150$  V, that emits energetic electrons. These primaries create trapped secondary electrons through ionizing collisions with added helium gas. Details of the apparatus and the diagnostics have been given elsewhere [3,4].

In the tokamak, Fig. 1, electrons with sufficiently low velocity parallel to the magnetic field are reflected by the mirror force and execute banana-like drift orbits. In the annular trap, the electrostatic force at the ends replaces the mirror force. There is in the tokamak a second class of particles not reflected by the mirror force, and collisions may cause particles to make transitions from one class of particles to the other. The annular trap, therefore, does not reproduce all of the transport features of the tokamak, but rather isolates for study the transport of trapped particles.

Axisymmetry results in conservation of azimuthal canonical angular momentum,  $P_\theta = r(qA_\theta + mv_\theta) = \text{const}$ , where  $A_\theta(r) = \frac{1}{2}rB_z$  is the vector potential for a uniform axial field, and  $q$  and  $m$  are the charge and mass of an electron, respectively. The azimuthal part of the velocity parallel to the magnetic field,  $v_\parallel B_\theta/B$ , changes sign at the ends of the drift orbit, and from conservation of  $P_\theta$ , the width of the drift orbit at the midplane is  $r_B = m(2v_\parallel/qB_z)(B_\theta/B)$ . This formula also applies to the banana width for the tokamak if  $B_z$  is interpreted as the poloidal field at the midplane [15]. The canonical angular momentum may be gyrophase and bounce averaged to obtain

$$P_\theta = r_0(mv_{D,\theta} + qA_\theta) = r_0\left(mv_{D,\theta} + \frac{1}{2}qr_0B_z\right), \quad (1)$$

where  $r_0$  is the radial location of the drift orbit center and  $v_{D,\theta}$  is the  $\theta$  component of the guiding center drifts. The torque from collisions,  $rF_\theta$ , changes the canonical angular momentum:

$$\begin{aligned} r_0F_\theta &= \frac{dP_\theta}{dt} \\ &= \frac{d}{dt}\left[r_0\left(mv_{D,\theta} + \frac{1}{2}qr_0B_z\right)\right] \cong r_0qB_z \frac{dr_0}{dt}, \end{aligned} \quad (2)$$

where we have used that  $r_0 \gg mv_{D,\theta}/qB_z$ .

The torque causing transport is the collisional drag on the equilibrium current  $\mathbf{J}$  which is determined from the fluid momentum equation

$$nm \frac{d\mathbf{v}}{dt} = -\nabla P - nq\nabla\Phi + \mathbf{J} \times \mathbf{B}, \quad (3)$$

where  $n$  is the number density,  $P$  is the scalar electron pressure, and  $\Phi$  is the electrostatic potential. The gradients

are radial except in the end regions which are ignored. The equilibrium current is

$$\mathbf{J} = \mathbf{B} \times (\nabla P + nq\nabla\Phi)/B^2 + \lambda\mathbf{B}, \quad (4)$$

where  $\lambda$  is an adjustable constant. In the case of a long mean free path, the axial confinement results in there being no fluid  $z$  velocity and hence no  $J_z$ . This condition constrains the choice of  $\lambda$ , and one finds that

$$J_\theta = \left[T \frac{dn}{dr} - nqE_r\right] / B_z, \quad (5)$$

where the gradient in the temperature (written in energy units) has been set to zero for simplicity. Collisions with neutrals create an azimuthal drag force on the equilibrium current,  $F_\theta = -mv_\theta\nu = -mJ_\theta\nu/nq$ , where  $\nu$  is the electron-neutral momentum transfer collision frequency. From Eq. (2), we find the radial particle flux  $\Gamma$ :

$$\begin{aligned} \Gamma &= n \frac{dr_0}{dt} = -(m\nu T/q^2B_z^2) \frac{dn}{dr} + n(m\nu/qB_z^2)E_r \\ &= -D_{\text{NC}} \frac{dn}{dr} + n\mu_{\text{NC}}E_r, \end{aligned} \quad (6)$$

where  $D_{\text{NC}} = m\nu T/q^2B_z^2$  is the neoclassical diffusion coefficient, and  $\mu_{\text{NC}} = m\nu/qB_z^2$  is the neoclassical mobility coefficient which relates the radial drift velocity to the radial electric field. In the limit of short mean free path, the adjustable constant in Eq. (4) is determined by a parallel Ohm's law. There being no parallel electric field (except in the end regions), the parallel current is zero and  $\lambda = 0$ . In this case, one finds the classical values for mobility,  $\mu_c = m\nu/qB^2$ , and for diffusion,  $D_c = m\nu T/q^2B^2$ . In these coefficients, the absolute value of  $B$  appears rather than  $B_z$ .

In the experiment, the confinement time resulting from mobility transport is measured rather than the mobility drift speed. We define a mobility confinement time,  $\tau_\mu$ , as the half-width of the plasma annulus divided by the mobility drift velocity:

$$\tau_\mu = dqB_z^2/\nu mE_r, \quad (7)$$

where  $d = (r_2 - r_1)/2$ . In order for mobility to be the dominant source of transport, this time scale must be made shorter than the diffusive time scale,  $d^2/D_{\text{NC}}$ . Comparison of these time scales shows that mobility transport is greater for  $|q|U \gg T$ . In the experiment,  $U = 36$  V and the measured initial electron temperature is 2.5 eV, thus this condition is satisfied initially. Experiments in which  $U$  has been varied from 18 to 90 V show linear scaling of the transport with  $U$ , which indicates that mobility is indeed dominant [4].

Numerical simulations of transport were performed by adding "Monte Carlo" collisions to a computer code solving the Lorentz equations of motion. The collisions reoriented the velocity vector randomly in the laboratory frame. Particles were launched midway between the cylinders and followed for 32 collision times. The time between collisions was made equal to approximately two bounce times

so that drift orbits were completed between collisions. Figure 2 shows the mean mobility drift speed for 96 particles for  $U = 36$  V and for different values of the axial and azimuthal fields. Also plotted is the drift velocity obtained from the neoclassical mobility in Eq. (6). The velocities obtained numerically vary inversely with  $B_z^2$  and are independent of  $B_\theta$ , which is the expected neoclassical scaling. A more complete simulation is impractical due to the large disparity between the time scales of gyration and of transport. The drift approximation cannot be used because diffusion of the guiding center is missed.

Experiments are performed by changing the filament bias potential to stop the filling of the trap and then recording the current drifting to the outer cylinder as a function of time. The current measured is the sum of the current of collected electrons and the current of the decaying image charge which is of the opposite sign and approximately half the magnitude. This factor of  $\frac{1}{2}$  arises from the image charge being divided between the inner and outer cylinders. The image charge decays in the same characteristic time as the density of confined electrons which creates the image charge, thus the image charge does not introduce a new time scale.

The collision frequency is determined from the pressure of helium added by means of a leak valve. An advantage of using helium is that the energy dependence of the collision frequency is weak. For example, at  $5 \times 10^{-5}$  Torr the collision frequency calculated from the momentum transfer cross section [16] is  $1.4 \times 10^5$  s $^{-1}$  both at 5 eV and at 15 eV. This is important because the electrons gain energy as they move toward the positively biased outer cylinder. The initial electron temperature has been determined from the retarding potential method and is approximately 2.5 eV [4]. The density determined from the charge collected at the outer cylinder, corrected for the effect of image charges, is  $2.4 \times 10^6$  cm $^{-3}$ . For  $B_z = B_\theta =$

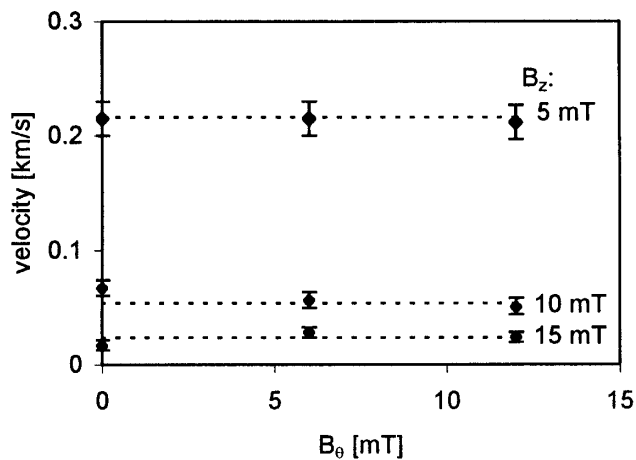


FIG. 2. The mobility drift velocity obtained from the simulations for different values of the axial and azimuthal fields. The velocities and error bars are from linear regressions made to the trajectories of 96 particles. The dotted lines are the drift velocities calculated from the neoclassical mobility. The simulation data show the neoclassical magnetic field dependence.

10 mT, the Larmor radius is 0.36 mm and the drift orbit width is 0.5 mm. The bounce frequency is  $3 \times 10^6$  s $^{-1}$  thus there are  $\sim 20$  bounces per collision and the particles are well within the neoclassical regime. The thermal velocity is  $9 \times 10^6$  m/s, the azimuthal electric drift is  $1.5 \times 10^5$  m/s, and the gradient and inertial drifts are  $\sim 10^4$  m/s.

The data in Fig. 3(a) are taken at a pressure of  $5 \times 10^{-5}$  Torr, with  $B_\theta = 0$  and with  $B_z$  from 10 to 17.5 mT. At the higher field, the decay occurs more slowly as a result of the decreased mobility. A logarithmic plot, Fig. 3(b), shows that the decay is approximately exponential for the first several  $e$  foldings and thus the  $e$ -folding time provides a convenient measure for the confinement time. A similar plot, in Fig. 3(c), shows the confinement times for an azimuthal field of 12 mT. Comparison of the two logarithmic

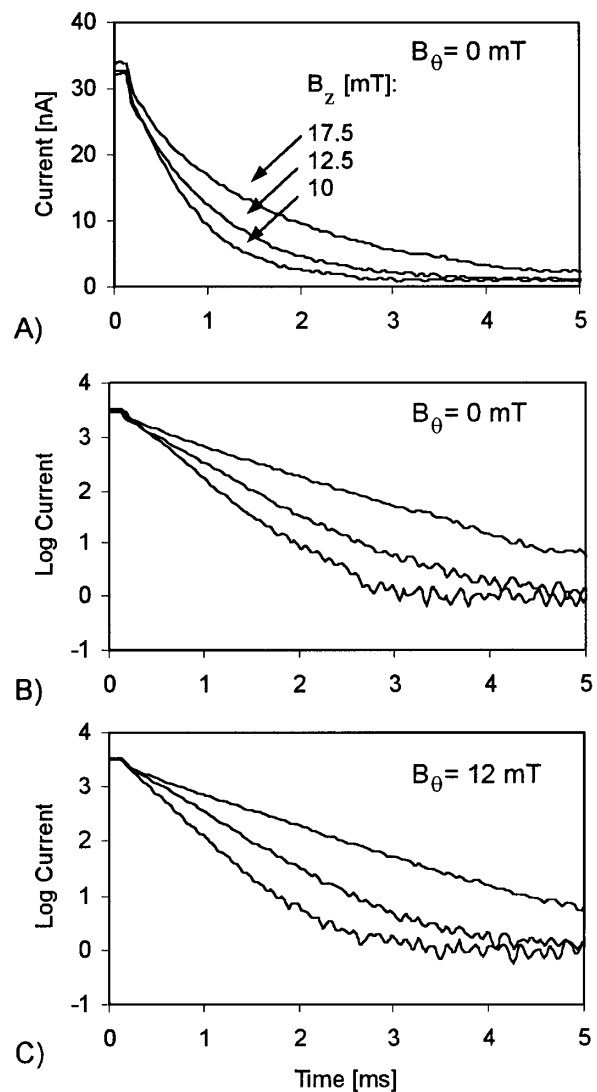


FIG. 3. (a) The current to the outer cylinder as a function of time at a helium pressure of  $5 \times 10^{-5}$  Torr for three values of axial field and with no azimuthal field. (b) Logarithmic plot of the same data. (c) Logarithmic plot for the conditions in (a) with an additional azimuthal field of 12 mT. The decay times are not changed by the addition of  $B_\theta$ .

plots shows that the mobility is very nearly independent of the azimuthal field.

Confinement times are plotted as a function of the square of the axial field in Fig. 4(a). The data are for five values of axial field from 7.3 to 17.5 mT and five values of azimuthal field from 0 to 12 mT. The solid line in this plot is 0.8 of the calculated confinement time from Eq. (7). This figure shows that the confinement time scales with the square of the axial field. The data points for different values of azimuthal field show no systematic variation with this field and lie nearly on top of one another. This point is shown more clearly in Fig. 4(b) in which the confinement times have been plotted as a function of azimuthal field. The data points lie near the lines given by 0.8 of the calculated confinement time from Eq. (7). The data are

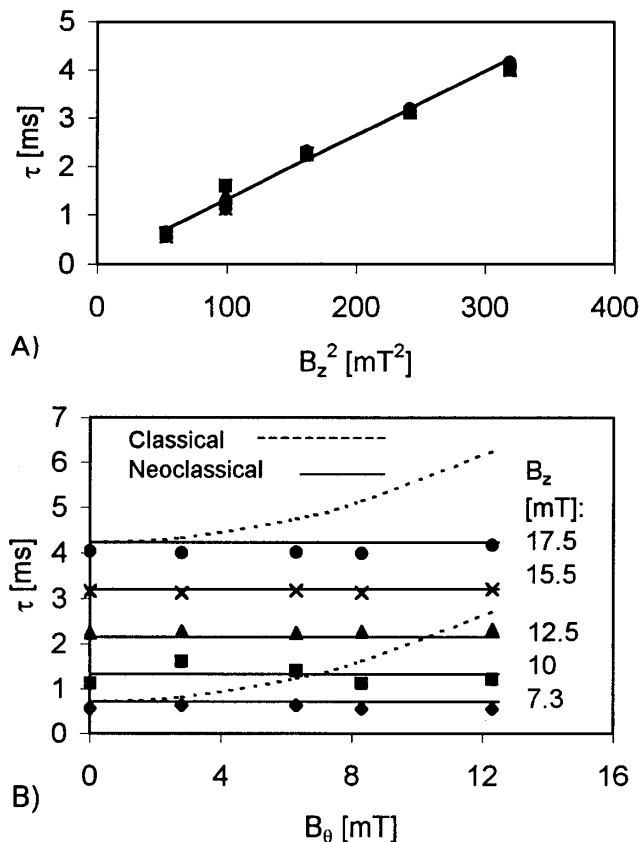


FIG. 4. (a) Plot of the measured confinement times as a function of the square of the axial field for values from 7.3 to 17.5 mT and azimuthal fields of 0, 3, 6.7, 8.7, and 12.3 mT. The pressure is  $2.5 \times 10^{-5}$  Torr. The points for different azimuthal fields lie nearly on top of one another. The line is 0.8 of the value calculated from Eq. (7). (b) Plot of the same data as in (a) as a function of the azimuthal field showing approximate agreement with 0.8 of the neoclassical time (solid lines) and disagreement with 0.8 of the classical time (dotted lines). The spread in the data points indicates the shot-to-shot reproducibility of the experiment.

clearly inconsistent with the classical prediction, the dotted lines in Fig. 4(b), because at the lowest value of axial field, 7.3 mT, the azimuthal field has been changed sufficiently (0–12 mT) for the classical mobility to have changed by a factor of 3.6. The measured confinement times being systematically low may be due to the somewhat arbitrary choice of half the annular width in the definition of  $\tau_\mu$  [Eq. (7)].

Experimental measurements of the neoclassical diffusivity should be possible if the experiment can be operated with a density sufficiently small for the mobility transport from the space charge electric field to be negligible. If the collision frequency were increased so that the mean free path becomes shorter than the length of the device, the mobility and diffusivity should make the predicted transition from the neoclassical value to the classical value. In the present device this is not possible because the high collision frequencies required result in a confinement time that is too short to be resolved by the diagnostics.

The authors acknowledge valuable discussions with John Cary, John Kline, Scott Parker, and Bob Walch and thank Matt Triplett for assistance in the construction of the experiment.

- [1] B. B. Kadomtsev and O. P. Pogutse, Nucl. Fusion **11**, 67 (1971).
- [2] F. L. Hinton and R. D. Hazeltine, Rev. Mod. Phys. **48**, 239 (1976).
- [3] S. Robertson and B. Walch, Rev. Sci. Instrum. **70**, 2993 (1999).
- [4] J. Kline, S. Robertson and B. Walch, in *Non-Neutral Plasma Physics III*, edited by J. J. Bollinger, R. L. Spencer, and R. C. Davidson, AIP Conf. Proc. Vol. 498 (AIP, New York, 1999), p. 290.
- [5] S. Robertson, Phys. Plasmas **4**, 2760 (1997).
- [6] J. H. Malmberg *et al.*, in *Non-Neutral Plasma Physics*, edited by C. W. Roberson and C. F. Driscoll, AIP Conf. Proc. Vol. 175 (AIP, New York, 1988), p. 28.
- [7] J. S. deGrassie and J. H. Malmberg, Phys. Fluids **23**, 63 (1980).
- [8] R. J. Taylor and L. Oren, Phys. Rev. Lett. **42**, 446 (1979).
- [9] R. J. Taylor *et al.*, Phys. Rev. Lett. **63**, 2365 (1989).
- [10] M. C. Zarnstorff and S. C. Prager, Phys. Fluids **29**, 298 (1986).
- [11] R. J. Hawryluk *et al.*, Phys. Plasmas **5**, 1577 (1998).
- [12] P. C. Efthimion *et al.*, Phys. Plasmas **5**, 1832 (1998).
- [13] B. W. Stallard *et al.*, Phys. Plasmas **6**, 1978 (1999).
- [14] Z. Lin, W. M. Tang, and W. W. Lee, Phys. Rev. Lett. **78**, 456 (1997).
- [15] K. Miyamoto, *Physics for Nuclear Fusion* (MIT Press, Cambridge, MA, 1979), Ch. 3. Note that in Eq. (3.100) the  $B_\theta$  is the poloidal  $B$ , not the azimuthal  $B$ .
- [16] J. L. Pack *et al.*, J. Appl. Phys. **71**, 5363 (1992).